

# Multiscale modeling for epitaxial growth

Russel E. Caflisch\*

**Abstract.** Epitaxy is the growth of a thin film on a substrate in which the crystal properties of the film are inherited from those of the substrate. Because of the wide range of relevant length and time scales, multiscale mathematical models have been developed to describe epitaxial growth. This presentation describes atomistic, island dynamics and continuum models. Island dynamics models are multiscale models that use continuum coarse-graining in the lateral direction, but retain atomistic discreteness in the growth direction. Establishing connections between the various length and time scales in these models is a principal goal of mathematical materials science. Progress towards this goal is described here, including the derivation of surface diffusion, line tension and continuum equations from atomistic, kinetic models.

**Mathematics Subject Classification (2000).** Primary 82D25; Secondary 82C24.

**Keywords.** Epitaxial growth, island dynamics, step edge, step stiffness, Gibbs–Thomson, adatom diffusion, line tension, surface diffusion, renormalization group, kinetic Monte Carlo.

## 1. Introduction

Epitaxy is the growth of a thin film on a substrate in which the crystal properties of the film are inherited from those of the substrate. Since an epitaxial film can (at least in principle) grow as a single crystal without grain boundaries or other defects, this method produces crystals of the highest quality. In spite of its ideal properties, epitaxial growth is still challenging to mathematically model and numerically simulate because of the wide range of length and time scales that it encompasses, from the atomistic scale of Ångströms and picoseconds to the continuum scale of microns and seconds.

The geometry of an epitaxial surface consists of step edges and island boundaries, across which the height of the surface increases by one crystal layer, and adatoms which are weakly bound to the surface. Epitaxial growth involves deposition, diffusion and attachment of adatoms on the surface. Deposition is from an external source, such as a molecular beam. Figure 1 provides a schematic illustration of the processes involved in epitaxial growth.

The models that are most often used to describe epitaxial growth include the following: A typical *Kinetic Monte Carlo* (KMC) method simulates the dynamics of

---

\*This work was partially supported by the National Science Foundation through grant DMS-0402276 and by the Army Research Office through grant DAAD19-02-1-0336

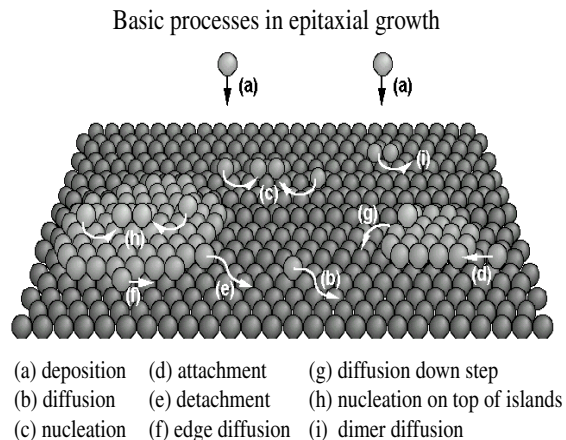


Figure 1. Schematic view of the processes involved in epitaxial growth.

the epitaxial surface through the hopping of adatoms along the surface. The hopping rate has the Arrhenius form  $e^{-E/kT}$  in which  $E$  is the energy barrier for going from the initial to the final position of the hopping atom. *Island dynamics* describe the surface through continuum scaling in the lateral directions but atomistic discreteness in the growth direction. *Continuum equations* approximate the surface using a smooth height function  $z = h(x, y, t)$ , obtained by coarse graining in all directions. Two other models are used to describe epitaxial growth on a limited time range. *Molecular dynamics* (MD) consists of Newton's equations for the motion of atoms on an energy landscape. Because the time scale for MD is femtoseconds ( $10^{-15}$  seconds), this can only be applied to very short time periods. *Rate equations* describe the surface through a set of bulk variables without spatial dependence. With some exceptions [5], [16], these have been used only for submonolayer growth.

The initial theories for epitaxial growth, such as [3], relied on an assumption that the system is close to equilibrium. In many epitaxial systems, however, the system is far from equilibrium so that a kinetic description is required. The emphasis in this article will be on KMC, island dynamics and continuum models for epitaxial systems that are far from equilibrium. A principal goal of mathematical materials science is to analyze the connections between these models. The results presented below, from the work of Margetis [18], Caflisch & Li [7], Margetis & Caflisch [19], Chua et al. [10], and Haselwandter & Vvedensky [14], [15] are for surface diffusion and step stiffness derived from atomistic kinetic models of epitaxy, and general continuum equations from a simplified model. These results are among the first of their kind; e.g., the formula for step stiffness comes from the first derivation of the Gibbs–Thomson formula from an atomistic, kinetic model rather than from a thermodynamic driving force. The results are far from complete. Other effects, such as the nonlinear terms in the continuum equations, have not been derived for a full model of epitaxy. In

addition, the derivations presented here are based on formal asymptotics, rather than rigorous mathematical analysis. Nevertheless, these results are a significant step toward a more complete theory and can serve as a starting point for more rigorous analysis.

For simplicity in the presentation, the lattice constant  $a$  will be taken to be  $a = 1$ , except in a few places where it is useful as a placeholder. Also, all transition rates (with units 1/time) are expressed in terms of equivalent diffusion constants (with units length<sup>2</sup>/time); i.e., a rate  $r$  is replaced by a diffusion coefficient  $D = a^2 r$ .

## 2. Mathematical models for epitaxial growth

In this section, various models for epitaxial growth are described, including atomistic KMC, island dynamics and continuum models, as well as a kinetic model for the structure of a step edge (or island boundary) that is used with island dynamics.

**2.1. Atomistic Models.** The simplest KMC model is a simple cubic pair-bond solid-on-solid (SOS) model [28], [29]. In this model, there is a stack of atoms, without vacancies, above each site on a two-dimensional lattice. New atoms are randomly deposited at a deposition rate  $F$ . Any surface atom (i.e., the top atom in the stack of atoms at a lattice point) is allowed to move to its nearest neighbor site at a rate  $r = D/a^2$  in which  $a$  is the lattice constant and  $D$  is a diffusion coefficient. In the simplest case,  $D$  is determined by

$$D = D_0 \exp\{-(E_S + nE_N)/k_B T\}. \quad (1)$$

In this equation,  $D_0$  is a constant prefactor of size  $10^{13} a^2 s^{-1}$ ,  $k_B$  is the Boltzmann constant,  $T$  is the surface temperature,  $E_S$  and  $E_N$  represent the surface and nearest neighbor bond energies, and  $n$  is the number of in-plane nearest neighbors. The terrace diffusion coefficient  $D_T$  for adatoms on a flat terrace and the edge diffusion coefficient  $D_E$  for adatoms along a step edge (with a single in-plane neighbor) are

$$D_T = D_0 \exp\{-E_S/k_B T\}, \quad (2)$$

$$D_E = D_0 \exp\{-(E_S + E_N)/k_B T\}. \quad (3)$$

Validity of this KMC model for epitaxial growth has been demonstrated by comparison to RHEED measurements from molecular beam epitaxy (MBE) experiments [11]. More complicated models for the diffusion coefficient, subject to the condition of detailed balance, are also used.

**2.2. Island dynamics models.** Burton, Cabrera and Frank [3] developed the first detailed theoretical description for epitaxial growth. This BCF model is an “island dynamics” model, since it describes an epitaxial surface by the location and evolution of the island boundaries and step edges. It employs a mixture of coarse graining and

atomistic discreteness, since island boundaries are represented as smooth curves that signify an atomistic change in crystal height.

Adatom diffusion on the epitaxial surface is described by a diffusion equation of the form

$$\partial_t \rho - D_T \nabla^2 \rho = F - 2(dN_{\text{nuc}}/dt) \quad (4)$$

in which  $F$  is the deposition flux rate and the last term represents loss of adatoms due to nucleation. Desorption from the epitaxial surface has been neglected.

The net flux to the step edge from upper and lower terraces is denoted as  $f_+ = f_+(y, t)$  and  $f_- = f_-(y, t)$ , respectively, in which

$$v\rho_+ + D_T \mathbf{n} \cdot \nabla \rho_+ = -f_+, \quad (5)$$

$$v\rho_- + D_T \mathbf{n} \cdot \nabla \rho_- = f_-. \quad (6)$$

The total flux is

$$f = f_+ + f_-. \quad (7)$$

Different island dynamics models are distinguished by having different formulas for the diffusive boundary conditions and normal velocity.

1. *The island dynamics model with irreversible aggregation:*

$$\begin{aligned} \rho &= 0, \\ v &= f. \end{aligned} \quad (8)$$

2. *The BCF boundary conditions:*

$$\begin{aligned} \rho &= \rho_*, \\ v &= f, \end{aligned} \quad (9)$$

in which  $\rho_*$  is the equilibrium adatom density at a step.

3. *The island dynamics model with step-edge kinetics:*

$$\begin{aligned} f_+ &= (D_T \rho_+ - D_E \phi) \cos \theta, \\ f_- &= (D_T \rho_- - D_E \phi) \cos \theta, \\ v &= k w \cos \theta, \end{aligned} \quad (10)$$

in which  $\phi$  and  $k$  are the densities of edge-atoms and kinks, and  $w$  is the kink velocity, defined in Section 2.3.

4. *The island dynamics model with line tension and surface diffusion:*

$$\begin{aligned} f_+ &= D_{d+}(\rho_+ - \rho_*) - \mu_+ \kappa, \\ f_- &= D_{d-}(\rho_- - \rho_*) - \mu_- \kappa, \\ v &= D_T \mathbf{n} \cdot [\nabla \rho] + \beta \rho_{*yy} + (\mu/D_E) \kappa_{ss}, \end{aligned} \quad (11)$$

in which  $\kappa$  is curvature and  $\kappa_{ss}$  is its second derivative along the length of a step edge,  $\rho_*$  is a reference adatom density,  $D_{d\pm}$  are the attachment/detachment rates, and  $\mu_{\pm} = (D_{d\pm}\rho_*/k_B T)\tilde{\gamma}$  in which  $\tilde{\gamma}$  is the step stiffness. This is further discussed in Section 4.

For the case of irreversible aggregation, a dimer (consisting of two atoms) is the smallest stable island, and the nucleation rate is

$$\frac{dN_{\text{nuc}}}{dt} = D\sigma_1\langle\rho^2\rangle, \quad (12)$$

where  $\langle\cdot\rangle$  denotes the spatial average of  $\rho(\mathbf{x}, t)^2$  and

$$\sigma_1 = \frac{4\pi}{\ln[(1/\alpha)\langle\rho\rangle D/F]} \quad (13)$$

is the adatom capture number. The parameter  $\alpha$  reflects the island shape, and  $\alpha \simeq 1$  for compact islands. Expression (12) for the nucleation rate implies that the time of a nucleation event is chosen deterministically. The choice of the location of the new island is determined by probabilistic choice with spatial density proportional to the nucleation rate  $\rho^2$ . This probabilistic choice constitutes an atomistic fluctuation that is retained in the island dynamics model [24].

Snapshots of the results from a typical island dynamics simulation are shown in Figure 2. Shown is the island geometry after coverage of 0.25 layers (left) and

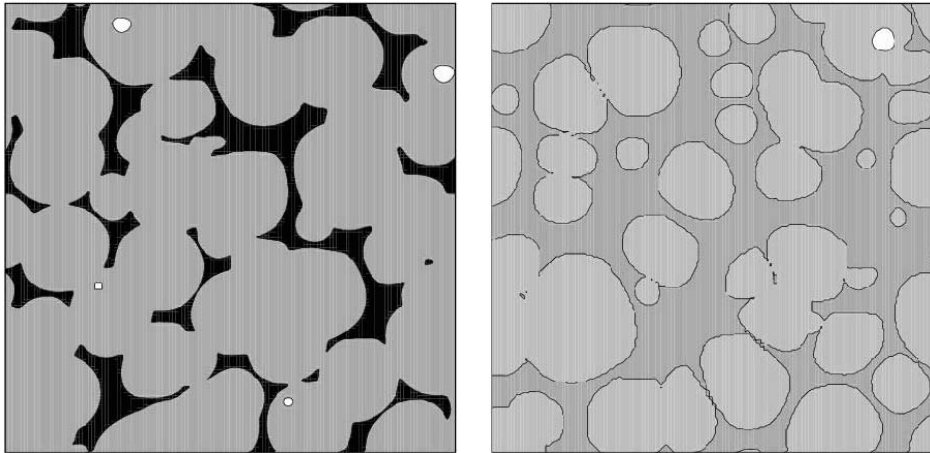


Figure 2. Island geometry for island dynamics with irreversible aggregation after deposition of 0.25 layers (left) and 10.25 layers (right).

coverage of 10.25 layers (right). These simulations are for irreversible aggregation with boundary conditions from Eq. (8). Numerical simulation of the island dynamics is performed using a level set method for thin film growth, as described in [4], [8].

Validation of the island dynamics/level set method has been performed by careful comparison to the results of the atomistic KMC models. Various generalizations and additional physics results are described in [22], [23]. Related work on level set methods for epitaxial growth are found in [9], [25], [26].

The principal dimensionless parameters for epitaxial growth are the ratios of flux and diffusive coefficients, which we refer to as “Péclet numbers” by analogy with fluid mechanics. Let  $\bar{f}$  be a characteristic size for the flux to an edge. Let  $P_T$  be the terrace Péclet number and  $P_E$  be the edge Péclet number, defined as

$$P_T = F/D_T, \quad (14)$$

$$P_E = \bar{f}/D_E, \quad (15)$$

in which  $D_E$  is the edge diffusion constant. Typical values for  $P_T^{-1} = D_T/F$  are in the range of  $10^4$  to  $10^8$ .

**2.3. The kinetic edge model.** The kinetic edge model of island dynamics was developed in [6]. It involves a statistical description of the crystalline structure of a step edge, including the edge-atom density  $\phi$  and the kink density  $k$ . Edge-atoms are atoms with a single in-plane neighbor along the step; kinks are atoms with two in-plane neighbors. Kinks are of two types – right-facing kinks and left-facing kinks – the densities of which are denoted by  $k_r$  and  $k_\ell$ . Figure 3 provides a schematic picture

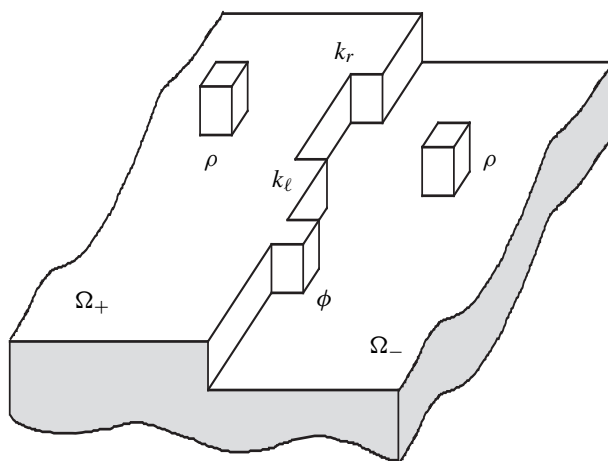


Figure 3. The geometry of step edge, showing adatoms with density  $\rho$  on the upper and lower terraces  $\Omega_+$  and  $\Omega_-$ , edge-atoms with density  $\phi$ , and right and left facing kinks with density  $k_r$  and  $k_\ell$ .

of the kink density model for a step edge. Related models have been derived by Balykov et al. [1], Balykov & Voigt [2] and Filimonov & Hervieu [13].

The kinetic edge model consists of a diffusion equation for the edge-atom density  $\phi$  and a convection equation for the kink density  $k$

$$\partial_t \phi - D_E \partial_s^2 \phi = f_+ + f_- - f_0, \quad (16)$$

$$\partial_t k + \partial_s (w(k_r - k_\ell)) = 2(g - h). \quad (17)$$

In Eq. (16),  $f_\pm$  are the net fluxes to the edge from terraces as defined in Eq. (5) and Eq. (6), and  $f_0$  is the net loss term due to the attachment of edge-atoms to kinks. In Eq. (17),  $w$  is the kink velocity, and  $g$  and  $h$  represent, respectively, the creation and annihilation of left-right kink pairs. Note that left-facing kinks and right-facing kinks move in opposite directions with velocity  $w$  and  $-w$ , respectively. The total kink density and the relation between the kink density and the normal angle [3] are

$$k_r + k_\ell = k, \quad (18)$$

$$k_r - k_\ell = \tan \theta. \quad (19)$$

The quantities  $f_+$ ,  $f_-$ ,  $f_0$ ,  $w$ ,  $g$ ,  $h$ , and  $v$  are determined by the following constitutive relations (in simplified form):

$$f_+ = (D_T \rho_+ - D_E \phi) \cos \theta, \quad (20)$$

$$f_- = (D_T \rho_- - D_E \phi) \cos \theta, \quad (21)$$

$$f_0 = v (\phi \kappa + 1), \quad (22)$$

$$w = l_1 D_E \phi + D_T (l_2 \rho_+ + l_3 \rho_-) = l_{123} D_E \phi + (l_2 f_+ + l_3 f_-) / \cos \theta, \quad (23)$$

$$\begin{aligned} g &= \phi (m_1 D_E \phi + D_T (m_2 \rho_+ + m_3 \rho_-)) \\ &= \phi (m_{123} D_E \phi + (m_2 f_+ + m_3 f_-) / \cos \theta), \end{aligned} \quad (24)$$

$$\begin{aligned} h &= k_r k_\ell (n_1 D_E \phi + D_T (n_2 \rho_+ + n_3 \rho_-)) \\ &= k_r k_\ell (n_{123} D_E \phi + (n_2 f_+ + n_3 f_-) / \cos \theta), \end{aligned} \quad (25)$$

$$X_t = v = w k \cos \theta, \quad (26)$$

where  $D_T$  is the (diffusion) hopping rate of an adatom on a terrace,  $D_E$  is the (diffusion) hopping rate of an edge-atom along or off an edge, and all  $l_i$ ,  $m_i$ ,  $n_i$  ( $i = 1, 2, 3$ ) are nonnegative numbers. The geometric parameters  $l_i$ ,  $m_i$ ,  $n_i$  count the number of paths from one state to another, cf. [6] for details. Here, these parameters are generalized to allow a factor relating the macroscopic density  $\rho$  or  $\phi$  to the local density of adatoms or edge atoms at a specific site. For convenience, we have used the notation

$$q_{ij} = q_i + q_j \quad \text{and} \quad q_{ijk} = q_i + q_j + q_k$$

for  $q = l, m$ , or  $n$ . For simplicity in this presentation, the constitutive laws (20)–(25) have been simplified by omission of terms that are insignificant for the kinetic steady state solutions of relevance to step-flow growth and by specialization to the case of  $\theta$  near 0. The terms omitted from (20)–(25) include terms that are important for detailed

balance, so that they are required for determination of the equilibrium solution for this model. In the more complete analysis of [6], [7], [19], all of the neglected terms are included.

There are several significant solutions for the kinetic step edge model Eq. (16)–Eq. (26). First, there is an equilibrium solution that was originally determined in [3] (note that some terms that have been omitted from the presentation here are significant for the equilibrium). Second there is a kinetic (i.e., nonequilibrium) steady state solution, for which the presentation includes all of the significant terms. Suppose that the kink density and edge Peclet number are small (i.e.,  $ak \ll 1$  and  $P_E \ll 1$ ) and that the step is symmetric (i.e.,  $\rho_+ = \rho_-$ ), then the adatom, edge-adatom and kink densities of the kinetic steady state are approximately

$$\rho = (D_E/D_T)a^{-1}\varphi, \quad (27)$$

$$\varphi = (16a/3)k^2, \quad (28)$$

$$k = \left(\frac{16}{15}P_E\right)^{\frac{1}{3}} a^{-1}. \quad (29)$$

The exponent  $1/3$  in (29) is related to the critical size for formation of a left-right kink pair. If the critical size were  $j$  (i.e., if  $j + 1$  edge-adatoms were required to form a stable kink pair) then the exponent would be  $j/(j + 2)$ .

Figure 4 shows a comparison of this steady state solution (solid line) and computational results from KMC (squares, circles and triangles) for kink density  $k$ . The

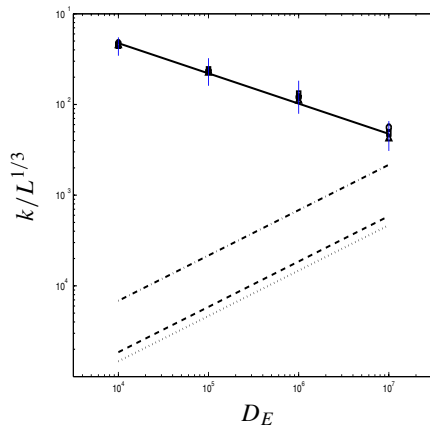


Figure 4. Kink density  $k$ , normalized by  $L^{1/3}$ , vs. edge diffusion coefficient  $D_E$  for kinetic steady state, for various values of terrace width  $L$ . Parameter values are flux  $F = 1$  and adatom diffusion  $D_T = 10^{12}$ . Results are shown from the kinetic theory (solid line) and KMC computations with  $L = 25$  (squares),  $L = 50$  ( $\circ$ ), and  $L = 100$  ( $\Delta$ ). These are compared to the corresponding equilibrium values for  $L = 25$  (dash-dotted line),  $L = 50$  (dashed line), and  $L = 100$  (dotted line), showing that the steady state and equilibrium differ both qualitatively and quantitatively.

BCF equilibrium values for  $k$  are also plotted (lower three lines) for comparison. In this figure,  $F = 1$  and  $D_T = 10^{12}$ , while  $D_E$  varies between  $10^4$  and  $10^7$ . The computations are for a periodic step train with straight steps at angle  $\theta = 0$  and with distance  $L = 25, 50,$  and  $100$  between the steps. The figure shows excellent agreement between the predictions of the present theory and the results of the KMC simulation, with differences that are less than one standard deviation of the KMC results. The results are significantly different from equilibrium both in size and in dependence on  $D_E$ .

**2.4. Continuum models.** Continuum models of epitaxial growth employ coarse graining in all directions. In most cases, they describe the epitaxial surface through a smooth height function  $z = h(x, y, t)$ . The general equation of this type, as discussed by Haselwandter and Vvedensky [14], [15], is

$$h_t = \nu_2 \nabla^2 h - \nu_4 \nabla^4 h + \lambda_{13} \nabla(\nabla h)^3 + \lambda_{22} \nabla^2(\nabla h)^2 + \xi \quad (30)$$

in which the  $\nu_2$  term comes from a height-dependence in the energy, the  $\nu_4$  term is surface diffusion, the  $\lambda$  terms are nonlinearities, and  $\xi$  is a stochastic noise term. This equation generalizes previous models, including the Edwards–Wilkinson (EW) equation with  $\nu_4 = \lambda_{13} = \lambda_{22} = 0$ , the Mullins–Herring (MH) equation with  $\nu_2 = \lambda_{13} = \lambda_{22} = 0$ , and the Villain–Lai–Das Sarma (VLDS) equation with  $\nu_2 = \lambda_{13} = 0$ . The relations between these models are further discussed in Section 5, through a renormalization group analysis applied to the Edwards–Wilkinson and Wolf–Villain models for epitaxial growth.

Derivation of these continuum equations has been mostly through symmetry arguments, thermodynamic driving force or by heuristics. The results reported in Sections 3 and 5 are among the first derivation of these equations from kinetic, atomistic models. Alternative modeling approaches have included additional dependent variables, not just the interface height. For example, Lo & Kohn [17] included adatom density in addition to height. Margetis et al. [20] derive similar results starting from an island dynamics model with a kinetic step edge description, as in Section 2.2 and 2.3.

### 3. Surface diffusion

As first derived by Mullins [21], the surface diffusion equation

$$h_t = -\nu_4 \nabla^4 h \quad (31)$$

describes the evolution of a surface through diffusion of the material that comprises the surface. Margetis [18] has given an atomistic, kinetic derivation of surface diffusion for epitaxial growth, and he found the surprising result that surface diffusion is not isotropic. While his derivation is based on detailed asymptotics starting from an island

dynamics model, the presentation here will be phenomenological but faithful to the spirit of Margetis's derivation.

Consider an epitaxial surface that consists of a series of steps that are nearly parallel. The terrace width  $\ell$  between steps is approximately  $\ell = a/|\nabla h|$  in which  $a$  is the lattice constant. Assume that the steps are slowly varying but widely spaced, so that  $a \ll \ell \ll \lambda$  in which  $\lambda$  is the length scale for the variation in the steps away from straight. Also, assume that edge diffusion coefficient  $D_E$  and the edge attachment/detachment rate  $D_d$  are much smaller than the terrace diffusion coefficient  $D_T$ .

The analysis is based on the following fundamental property of diffusion: Consider a composite consisting of strips of two material with diffusion coefficients  $D_1$  and  $D_2$  and with strip widths  $a_1$  and  $a_2$ . The effective diffusion coefficient  $D_*$  for the composite is the arithmetic average if the diffusion is in the direction along the strips (i.e., a parallel configuration) and it is the harmonic average if the diffusion is in the direction perpendicular to the strips (i.e., a series configuration); i.e.,

$$D_* = \begin{cases} (a_1 D_1 + a_2 D_2)/(a_1 + a_2) & \text{parallel configuration,} \\ ((a_1 D_1^{-1} + a_2 D_2^{-1})/(a_1 + a_2))^{-1} & \text{series configuration.} \end{cases} \quad (32)$$

Define a tangential variable  $s$  along the steps and a normal variable  $n$  perpendicular to the steps. In the tangential direction, adatoms diffuse at the terrace diffusion rate of  $D_T$  on the terraces between steps and at the edge diffusion rate  $D_E$  along the steps. Since the terraces and steps are in parallel in the tangential direction, the corresponding diffusion coefficient

$$D_{ss} = (a D_E + \ell D_T)/(a + \ell) \approx D_T. \quad (33)$$

Diffusion of adatoms normal the steps is also at rate  $D_T$ , but it is interrupted by attachment and detachment from the steps at rate  $D_d$ . Since the terraces and steps are in a series configuration in the normal direction  $n$ , the diffusion coefficient in this direction is

$$D_{nn} = ((2a D_d^{-1} + \ell D_T^{-1})/(a + \ell))^{-1} \approx D_T (1 + m|\nabla h|)^{-1} \quad (34)$$

in which

$$m = 2D_T/D_d. \quad (35)$$

The factor of 2 in the last two formulas is due to the details of the attachment/detachment model used in [18].

Now follow the derivation of diffusion from the thermodynamic driving force (but note that Margetis used a perturbation expansion based on the kinetic equations rather than this near-equilibrium argument). The evolution of the height  $h$  is given in terms of the mobility tensor  $M$ , current  $j$  and chemical potential  $\mu$  as

$$\begin{aligned} h_t &= -\nabla \cdot j \\ &= \nabla \cdot (M \nabla \mu) \end{aligned} \quad (36)$$

since  $j = -M\nabla\mu$  and  $\mu = \delta E/\delta h = -g_1\nabla \cdot (\nabla h/|\nabla h|) - g_3\nabla h \cdot (|\nabla h|\nabla h)$ . By the argument above,  $M$  is the matrix

$$M = \frac{D_T\rho_*}{K_B T} \begin{pmatrix} 1 & 0 \\ 0 & (1 + m|\nabla h|)^{-1} \end{pmatrix} \tag{37}$$

in the  $n, s$  coordinates.

#### 4. Step stiffness

In [7], Cafilisch and Li considered the zero limit of the edge Peclet  $P_E$  number for the kinetic edge model from Section 2.3 for a step that is a slight perturbation of a straight step with  $\theta = 0$ , i.e., parallel to a crystallographic direction. They used a very specific form for the wavelength and amplitude of the perturbation and their scaling with  $P_E$ , and they assumed that the solution was close to the kinetic steady state Eq. (29) for  $\theta = 0$ . They derived the boundary conditions Eq. (11) for the evolution of a step, including the Gibbs–Thomson form of the step stiffness and a term due to edge diffusion of the adatoms that attach to the step.

More recently, Margetis and Cafilisch [19] performed a more general analysis for a step with variable  $\theta$ . Under the assumption that  $P_E \ll 1$  and that the solution is close to the kinetic steady state, they identified several regimes for the behavior of the solution and the step stiffness coefficient. Since the complete results are complicated, we present the results in an abbreviated form and refer to [19] for a detailed expression.

First, suppose that the curvature  $\kappa$  of the step satisfies

$$|\kappa| < O(P_E) \ll 1. \tag{38}$$

Then the step edge kinetics allow for two regimes for the step stiffness  $\tilde{\gamma}$ :

$$\tilde{\gamma} = \begin{cases} (k_B T/D_T\rho_*)\theta^{-1} & \text{for } P_E^{1/3} \ll \theta \ll 1, \\ (k_B T/D_T\rho_*)\tilde{\gamma}_0 & \text{for } 0 < \theta \ll P_E^{1/3}. \end{cases} \tag{39}$$

The results for step stiffness imply results for the line tension  $\gamma$ , since  $\tilde{\gamma} = \gamma + \gamma_{\theta\theta}$  then to leading order

$$\gamma \approx \begin{cases} (k_B T/D_T\rho_*)\theta \log \theta & \text{for } P_E^{1/3} \ll \theta \ll 1, \\ c_0 & \text{for } 0 < \theta \ll P_E^{1/3}. \end{cases} \tag{40}$$

in which  $c_0$  is an undetermined constant. In the outer solution,  $\gamma_{\theta}$  is nearly infinite for  $\theta$  small, which predicts a flat facet corresponding to  $\theta = 0$ . The inner solution provides some curvature to this facet, however. These results are consistent with the recent results of Stasevich et al. [27] for the step stiffness in an Ising model.

## 5. Coarse graining

In a remarkable series of papers [10], [14], [15], Chua et al. and Haselwandter & Vvedensky performed coarse-graining, followed by a renormalization group analysis, for the Edwards–Wilkinson [12] and Wolf–Villain [30] models of epitaxial growth. In the Wolf–Villain model, particles are randomly deposited on the surface at rate  $F$ . Instead of diffusing along the surface, however, each deposited particle makes a single hop to the nearest neighbor site that has the largest number of neighbors (i.e., the highest coordination), or stays where it landed if that hop does not increase the number of neighbors. In two-dimensions (i.e., a one dimensional surface), a particle hops to a position that is no higher than its original position, while in three-dimensions, some particles may increase their coordination by hopping to a higher position.

For a general lattice model, Haselwandter and Vvedensky first write the stochastic evolution in terms of a Chapman–Kolmogorov transition probability  $T_t(H_2|H_1)$  for transition between height configuration  $H_1$  to  $H_2$  in time  $t$

$$T_{t+t'}(H_3|H_1) = \sum_{H_2} T_{t'}(H_3|H_2)T_t(H_2|H_1). \quad (41)$$

This can be converted to a Master equation

$$P(H, t) = \sum_r [W((H-r); r)P(H-r, t) - W(H; r)P(H, t)] \quad (42)$$

in which  $P(H, t)$  is the probability for height configuration  $H$  at time  $t$ ,  $W(H; r)$  is the transition rate between  $H$  and  $H+r$ , and  $r$  is the array of jump lengths between configurations. They then apply a Kramers–Moyal–van Kampen expansion with “largeness” parameter  $\Omega$ , with the lattice size and time between depositions being proportional to  $\Omega^{-1}$ . In the limit  $\Omega \rightarrow \infty$ , this expansion yields a lattice Langevin equation

$$\partial h_{ij}/\partial t = K_{ij}^{(1)} + \eta_{ij} \quad (43)$$

in which  $K_{ij}^{(1)}$  are the first moment of the transition rates and  $\eta_{ij}$  are Gaussian noises with mean zero and covariances given by the second moment of the transition rates. After performing a smoothing and a cutoff Taylor expansion and specializing to the Wolf–Villain (or Edwards–Wilkinson) model, the Langevin equation becomes Eq. (30).

Finally they perform a renormalization group (RG) analysis of equation Eq. (30). In the RG “flow”, length and time are scaled at an exponential rate in the flow variable  $\ell$ . This analysis shows that the RG fixed points consist of the EW, MH and VLDS equations, as well as three previously unrecognized fixed points. The significance of this result is that as the solution of Eq. (30) evolves, it will linger near the fixed points, so that the solution will approximate a solution of each of these equations. The most important of the equations corresponding to these new fixed points, is their “FP1”.

Although it is complicated in general, in the two dimensional case it has the form

$$h_t = -|\nu_2|\nabla^2 h - |\nu_4|\nabla^4 h - |\lambda_{13}|\nabla(\nabla h)^3 + \lambda_{22}\nabla^2(\nabla h)^2 + \xi \quad (44)$$

which should be compared to Eq. (30). In two-dimensions this equation corresponds to a stable fixed point, but the corresponding equation in three dimensions corresponds to an unstable fixed point for the RG flow. This coarse graining and RG analysis provides both a derivation of these equations, starting from the EW or WV model, as well as an indication of the regimes of their validity.

**Acknowledgments.** The presentation here benefitted from discussions with Ted Einstein, Christoph Haselwandter, Dionisios Margetis, Tim Stasevich, Axel Voigt, and Dimitri Vvedensky. In particular, Margetis, Haselwandter and Vvedensky provided the author with advance copies of their unpublished work.

## References

- [1] Balykov, L., Kitamura, M., Maksimov, I. L., Nishioka, K., Kinetics of non-equilibrium step structure. *Phil. Mag. Lett.* **78** (1998), 411–418.
- [2] Balykov, L., Voigt, A., Kinetic model for step flow growth of [100] steps. *Phys. Rev. E* **72** (2005), #022601.
- [3] Burton, W. K., Cabrera, N., Frank, F. C., The growth of crystals and the equilibrium structure of their surfaces. *Phil. Trans. Roy. Soc. London Ser. A* **243** (1951), 299–358.
- [4] Caffisch, R. E., Gyure, M. F., Merriman, B., Osher, S., Ratsch, C., Vvedensky, D. D., Zinck, J. J., Island dynamics and the level set method for epitaxial growth. *Appl. Math. Lett.* **12**, 13 (1999), 13–22.
- [5] Caffisch, R. E., Meyer, D., A reduced order model for epitaxial growth. *Contemp. Math.* **303** (2002), 9–23.
- [6] Caffisch, R. E., E, W., Gyure, M. F., Merriman, B., Ratsch, C., Kinetic model for a step edge in epitaxial growth. *Phys. Rev. E* **59** (1999), 6879–6887.
- [7] Caffisch, R. E., Li, B., Analysis of island dynamics in epitaxial growth. *Multiscale Model. Sim.* **1** (2002), 150–171.
- [8] Chen, S., Kang, M., Merriman, B., Caffisch, R. E., Ratsch, C., Fedkiw, R., Gyure, M. F., Osher, S., Level set method for thin film epitaxial growth. *J. Comp. Phys.* **167** (2001), 475–500.
- [9] Chopp, D., A level-set method for simulating island coarsening. *J. Comp. Phys.* **162** (2000), 104–122.
- [10] Chua, A. L.-S., Haselwandter, C. A., Baggio, C., Vvedensky, D. D., Langevin equations for fluctuating surfaces. *Phys. Rev. E* **72** (2005), #051103.
- [11] Clarke, S., Vvedensky, D. D., Origin of reflection high-energy electron-diffraction intensity oscillations during molecular-beam epitaxy: A computational modeling approach. *Phys. Rev. Lett.* **58** (1987), 2235–2238.

- [12] Edwards, S. F., Wilkinson, D. R., The surface statistics of a granular aggregate. *Proc. Roy. Soc. Ser. A* **381** (1982), 17–31.
- [13] Filimonov, S. N., Hervieu, Y. Y., Terrace-edge-kink model of atomic processes at the permeable steps. *Surface Sci.* **553** (2004), 133–144.
- [14] Haselwandter, C. A., Vvedensky, D. D., Multiscale theory of fluctuating interfaces during growth. Preprint, 2005.
- [15] Haselwandter, C. A., Vvedensky, D. D., Multiscale theory of fluctuating interfaces: From self-affine to unstable growth. Preprint, 2005.
- [16] Kariotis, R., Lagally, M. G., Rate equation modelling of epitaxial growth. *Surface Sci.* **216** (1989), 557–578.
- [17] Lo, T. S., Kohn, R. V., A new approach to the continuum modeling of epitaxial growth: slope selection, coarsening, and the role of the uphill current. *Physica D* **161** (2002), 237–257.
- [18] Margetis, D., Unified continuum approach to crystal surface morphological relaxation. Preprint, 2005.
- [19] Margetis, D., Caflisch, R. E., Modified kinetic model of step edge dynamics: modeling and derivation of step stiffness. Preprint, 2005.
- [20] Margetis, D., Voigt, A., Caflisch, R. E., private communication, 2005.
- [21] Mullins, W., Theory of thermal grooving. *J. Appl. Phys.* **28** (1957), 333–339.
- [22] Petersen, M., Ratsch, C., Caflisch, R. E., Zangwill, A., Level set approach to reversible epitaxial growth. *Phys. Rev. E* **64** (2001), #061602.
- [23] Ratsch, C., Gyure, M., Caflisch, R. E., Gibou, F., Petersen, M., Kang, M., Garcia, J., Vvedensky, D. D., Level-set method for island dynamics in epitaxial growth. *Phys. Rev. B* **65** (2002), #195403.
- [24] Ratsch, C., Gyure, M. F., Chen, S., Kang, M., Vvedensky, D. D., Fluctuations and scaling in aggregation phenomena. *Phys. Rev. B* **61** (2000), 10598–10601.
- [25] Russo, G., Smereka, P., A level-set method for the evolution of faceted crystals. *SIAM J. Sci. Comput.* **21** (2000), 2073–2095.
- [26] Smereka, P., Spiral crystal growth. *Physica D* **138** (2000), 282–301.
- [27] Stasevich, T. J., Gebremariam, H., Einstein, T. L., Giesen, M., Steimer, C., Ibach H., Low-temperature orientation dependence of step stiffness on {111} surfaces. *Phys. Rev. B* **71** (2005), #245414.
- [28] Vvedensky, D. D., Atomistic modeling of epitaxial growth: comparisons between lattice models and experiment. *Comp. Materials Sci.* **6** (1996), 182–187.
- [29] Weeks, J. D., Gilmer, G. H., Dynamics of crystal growth. *Adv. Chem. Phys.* **40** (1979), 157–228.
- [30] Wolf, D. E., Villain, J., Growth with surface diffusion. *Europhys. Lett.* **13** (1990), 389–394.

Mathematics Department, UCLA, Los Angeles, CA 90095-1555, U.S.A.

E-mail: Caflisch@math.ucla.edu